Tactile Object Exploration using Cursor Navigation Sensors

M. Kjærgaard, D. Kraft,
H. Petersen and N. Krüger
Maersk Mc-Kinney Moller Institute
University of Southern Denmark
Odense, Denmark
{mortenkj,kraft,hgp,norbert}@mip.sdu.dk

A. Bierbaum, T. Asfour
and R. Dillmann
Institute of Computer Science and Engineering
University of Karlsruhe (TH)
Karlsruhe, Germany
{bierbaum,asfour,dillmann}@ira.uka.de

***Abstract*— In robotic applications tactile sensor systems serve the purpose of localizing a point of contact and measuring contact forces. We have investigated a novel variant of a classic tactile sensor, the Force Sensing Resistor (FSR), which is commonly used in cursor navigation technology. We show the potential of this sensor for active haptic exploration. More specifically, we present experiments and results which demonstrate the extraction of relevant object properties such as local shape, weight and elasticity using this technology.**

An interesting aspect of this sensor is that beside a localization of contact points and measurement of the contact normal force also shear forces can be measured which is relevant for surface normal estimation and weight measurements. Scalable tactile sensor arrays have been developed with this sensor which can be arranged as tiles on a surface, e.g. a manipulator.

I. Introduction

By means of tactile sensing haptic information about an object is acquired during a physical contact between sensor and object. Tactile sensors offer exciting possibilities for use in mechatronic devices and measuring instruments in many areas of science and engineering (see, e.g., [1]).

In this work, we introduce a tactile sensor framework for grasp control and haptic exploration with different robot platforms (e.g., with an industrial robot equipped with a two-jaw gripper and with the humanoid robot platform ARMAR-III [2]) that deploys technology commonly used for cursor navigation on, e.g., laptops. The sensor system is based on available touch sensors involving FSR-technology [3] to acquire the directional contact force vector and the contact location. This type of sensor has originally been developed as cursor navigation input device for hand-held devices. It is therefore low cost and off-the-shelf available. Also, the sensors only need few additional electronic components for embedded integration and there are sufficiently versatile to be applied to manipulators of different geometries.

A comprehensive overview about tactile sensing technology can be found in [1], and more recently in [4] and [5]. It is distinguished between intrinsic sensors, which measure forces internal to the manipulator mechanics, e.g. via load cells at actuation joints, and extrinsic tactile sensors. The latter ones measure forces applied to the manipulator surface and can be found as distributed individual sensors or as dense sensor arrays, which can locate the point of contact on the sensor surface. The contact force itself is derived indirectly by measuring capacity or resistance of the physical sensing element. In Force Sensing Resistors (FSR) [6], a piezoresistive material is used, which varies its electrical resistance in response to an applied mechanical load. Further, there exist also some sensor designs which determine contact force by measuring deformations of the sensor surface with optical sensors [7], [8].

For the purpose of grasp control and shape exploration, measurement of the directional force vector (normal force and shear) and of the contact location is required [9]. The first type of information is usually obtained through load cells in manipulator joints, but it is not possible to also determine the point of contact in multi-contact situations with this type of sensor. For this purpose additional extrinsic tactile sensor arrays are required. New sensor designs for determining both types of information equally are under investigation [10], [11] but have not been shown in an robotic application yet. Further, the latter sensors currently do not provide the dynamic range required in standard robotic grasping or haptic exploration.

We see the technology developed in the context of cursor navigation as an interesting option also for tactile sensing due to its low cost, richness of information (position, normal and shear force) and its modularity. We show the potential of this sensor for active haptic exploration. In particular, we present experiments and results which demonstrate the extraction of relevant object properties such as local shape, weight and elasticity with this technology.

This paper is structured as follows. In the next section the relevant details of the tactile sensor system are described. This includes a description of the sensor characteristics and the proposed calibration method. In section III, we present experiments on the extraction of haptic object properties such as local shape, weight and elasticity. Finally we give a conclusion and an outlook on our future work in section IV.

II. Tactile sensor system

The sensing element of our tactile sensor system is the *MicroNav* cursor navigation sensor from Interlink Electronics [12], which is a four-quadrant FSR sensor. Fig. 1(a) depicts the layout of this sensor element with its four subsensors, labeled N, E, S, W in correspondence to the compass orientations. The sensor element comes in a Surface Mounted

Preprint submitted to 2008 IEEE International Conference on Robotics and Automation. Received September 14, 2007.

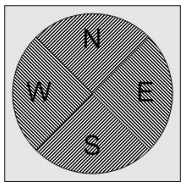

(a) MicroNav sensor layout.

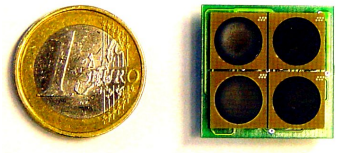

(b) Integrated quadruple sensor array module and 1 Euro coin.

Fig. 1. Tactile sensor.

Device (SMD) package with dimensions $10\times10\times1.4$ mm, the solderable contacts are situated at the bottom side.

The electrical integration is realized with a voltage divider circuit and an Analog-Digital-Converter (ADC) for acquiring the measurement signal as proposed in [6]. Fig. 1(b) shows our realization of a four sensor array module. The sensor module has 16 independent tactile sensing points. By arranging several modules in a dense matrix structure a spatial resolution of 5 mm can be achieved. A microcontroller with integrated ADC, RS232 communication and CAN bus interface is located at the bottom side of the circuit board. With the CAN bus it is possible to interconnect up to 256 individual array boards for realizing a modular tactile sensing system, while the standard RS232 interface is suitable for easily connecting a sensor module to a standard PCs serial interface.

The sensing plane of the *MicroNav* is not supposed to be actuated directly but needs an elastic actuation tip, which both protects the sensor surface and distributes an applied force across the element. For the setup and experiments described we used a rubber actuation tip similar to the reference design [12], see Fig. 2(a).

Fig. 2(b) shows an individual *MicroNav* sensor embedded in the silicon rubber actuation tip of a finger in an anthropomorphic hand [13] for the humanoid robot ARMAR-III, a configuration which is still under investigation.

Characteristics of the sensor

Although FSR sensors are not recommended for precision measurement devices due to their production tolerance ranging from 15% - 25% and their long term settling characteristics, it is possible to calculate a contact force value from the resistance measurement using a calibration procedure.

It should also be noted that FSRs need a minimum force applied for sensing, the so called break force, which limits the measurement range at the lower end. The exact value depends on mechanical characteristics of the sensor and may be adjusted by design of the actuation tip. A typical value for the sensor used is about 0.2 N.

In our calibration setup a single sensor element was mounted to one finger of the parallel gripper of an industrial robot arm. While moving the sensor perpendicular towards the sensitive measurement area of a digital scale, which was used for force measurement here, simultaneous readings of force and sensor output at different pressure levels could be acquired in a measurement sequence.

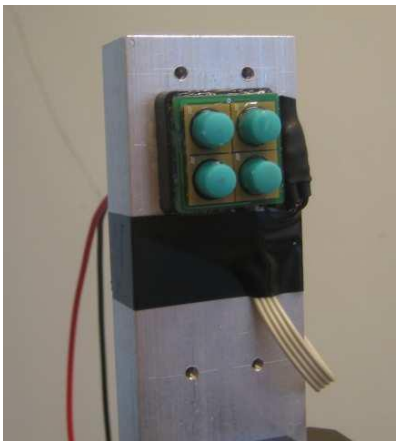

(a) Sensor array with actuation tips mounted to a gripper.

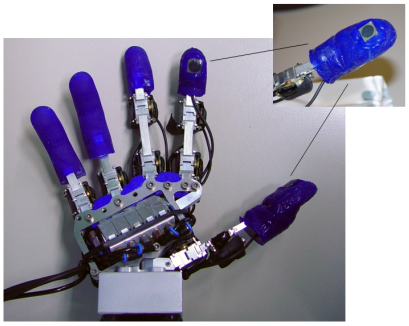

(b) Single sensor integrated in the finger tip of an anthropomorphic robot hand.

Fig. 2. Different applications of the sensor.

An exemplar measurement of all four subsensors is shown in Fig. 3. It shows that the relationship between force and conductivity of a sensor is not completely linear over the measured range. In the low-force range it is possible to approximate the relationship using a first order function. This will not give the same accuracy as a more complex function but still the result is sufficient for our application of tactile object exploration as we will mainly operate the sensor in this measurement range. It should be noted that since the characteristics of FSR sensors usually differ from part to part, individual calibration is required in general to achieve maximum accuracy.[1]

Because of the intended application measurement values above 4 N will be disregarded in the following. The remaining datapoints were approximated to a straight line using least-squares estimation as illustrated in Fig. 3. It was found sufficient for the application to use a common

[1]Note that the graph representing the W sub-sensor in Fig. 3, is growing clearly faster than the remaining three sub-sensors. Further investigation revealed, that this effect comes from a tangential force component acting upon the sensor tip, which in turn leads to a torque applied to the sensing area. In the future, this problem could be eliminated by reducing height and rotational elasticity of the actuation tip.

Preprint submitted to 2008 IEEE International Conference on Robotics and Automation. Received September 14, 2007.

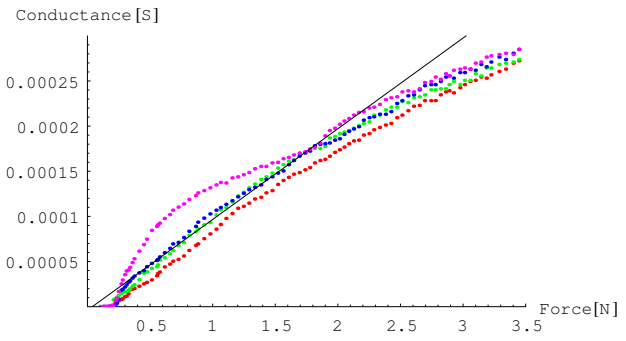

Fig. 3. Measured conductance from all sensors during linearization experiment. Red=N, Blue=S, Green=E, Purple=W

force-conductance relationship for all sensors during our experiments and not to apply individual calibration.

III. Extraction of Haptic Object Properties

For evaluation of the sensor system described above we have performed experiments related to the exploration of various haptic object features. For the experiments one tactile sensor array module was mounted on each finger of the parallel gripper of a *Stäubli Scara* series 6 axis industrial manipulator. For the surface exploration experiments described in Sections III-A and III-B only one finger of the gripper was used, while both fingers were in operation for the experiments in Sections III-C and III-D involving grasping. A dedicated control program on a PC was implemented for each experiment.

The measurement from a sensor element is a four dimensional force vector $\overrightarrow{S}$ consisting of the force measurements from each subsensor

$$\overrightarrow{S} = \begin{pmatrix} n \\ s \\ w \\ e \end{pmatrix} \quad .$$

From this we define a contact force vector

$$\overrightarrow{P} = \begin{pmatrix} n-s \\ w-e \end{pmatrix} \cdot \frac{1}{|\overrightarrow{S}|} \quad .$$

A. Surface normals with single Sensors

The knowledge of the surface normal is an important information in addition to point of contact and force amplitude since it allows for characterizing the shape of objects more precisely. It gives also important information about the stability of a grasp and how to align the grasping device optimally to the object.

In the following experiment we studied the performance of a single *MicroNav* sensor to acquire the orientation of a touched surface, which is directly related to the contact normal force vector.

Instead of describing the contact surface orientation by its normal vector we chose to describe it by two angles, the tilt angle α and the roll angle β, which allows for easier interpretation and qualification of the measurement results.

Fig. 4(b) shows the definition of the tilt angle. A tilt angle of $\alpha = 0$ means the sensor is normal to the surface it is in contact with, and a positive tilt angle means the sensor is tilted towards the N direction. Fig. 4(c) shows the direction of the roll angle. A roll angle of $\beta = 0$ gives a positive tilt in the N direction, $\beta = \frac{\pi}{2}$ gives a tilt in the W direction and so on.

Applying ranges of $\alpha \in \left\{-\frac{\pi}{2}, +\frac{\pi}{2}\right\}$ and $\beta \in \{0, \pi\}$ all possible orientations of a surface relative to the sensor actuation tip can be represented.

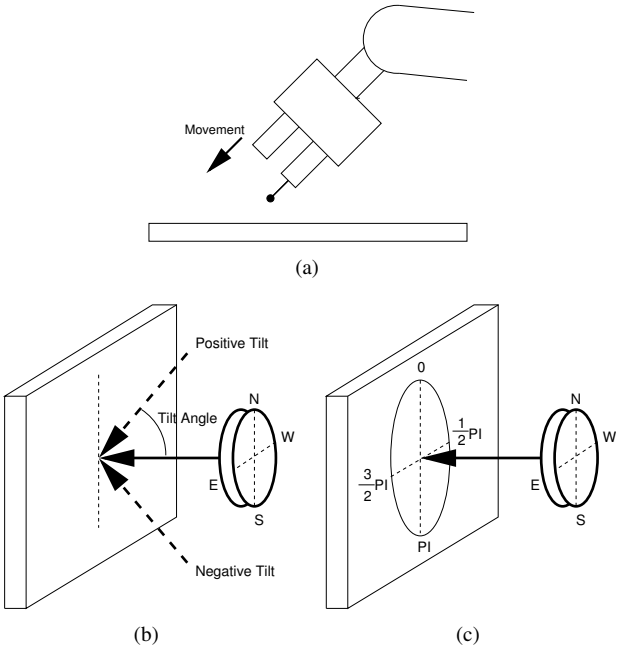

Fig. 4. **(a)** Direction of the robot movement in the experiments. **(b)** Surface orientation defined by tilt angle α. **(c)** Surface orientation defined by roll angle β.

Now all combinations of the following roll and tilt angles were tested by touching a table surface within the workspace of the robot arm:

$$\alpha \in \left\{0, \frac{1}{32}\pi, \frac{2}{32}\pi, \frac{3}{32}\pi, \frac{4}{32}\pi, \frac{5}{32}\pi, \frac{6}{32}\pi\right\}$$
$$\beta \in \left\{0, \frac{1}{6}\pi, \frac{2}{6}\pi, \frac{3}{6}\pi\right\}$$

Every pair of angles was tested six times to collect information about mean value and standard deviation. A graphical representation of the results is shown in Fig. 5, where the $\overrightarrow{P}$-components are drawn versus the applied tilt angle.

The results show that the components of $\overrightarrow{P}$ from the sensor measurement depend on both the roll and the tilt angle. From the measurements the applied tilt angle can be derived up to a value of about $0.4\,rad$ (22°) without becoming ambiguous.

Preprint submitted to 2008 IEEE International Conference on Robotics and Automation. Received September 14, 2007.

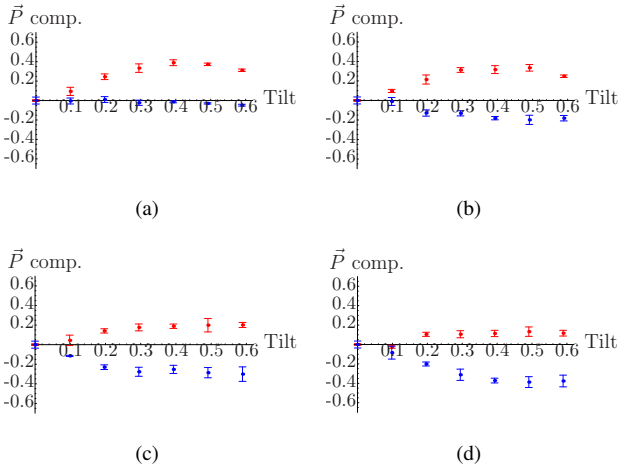

Fig. 5. Results from surface normal experiment using the *MicroNav* sensor. Mean values of $\vec{P}$ shown for the tested tilt angles. The tilt angle is given in radian. Red=North/South axis, Blue=East/West axis. **(a)** For a roll angle $\beta = 0$. **(b)** For a roll angle $\beta = \frac{1}{6}\pi$. **(c)** For a roll angle $\beta = \frac{2}{6}\pi$. **(d)** For a roll angle $\beta = \frac{3}{6}\pi$.

B. Active Surface Exploration

Further, we wanted to investigate the performance of the sensor in shape extraction from haptic data. For this purpose we derived a shape exploration algorithm from the contour follower proposed in [14]. The details of the algorithm are given in the appendix .

For the experiment, a bowl (see Fig. 6) was placed upside down and fixed within the workspace so the robot could press a finger with the sensor array against the surface without moving the bowl. Initially, the controller program needs to be provided with location and orientation of a point on the surface of the bowl as starting point.

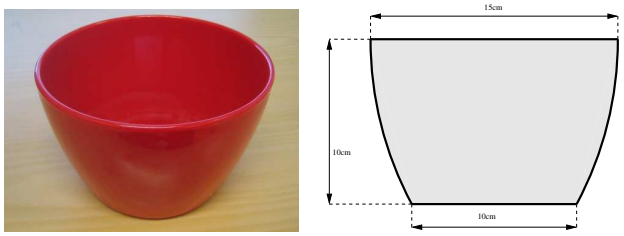

Fig. 6. **a)** The plastic bowl used in the exploration experiment. **b)** The dimensions of the bowl.

During the exploration it was visible that the robot properly aligned the sensor array with the surface. The points found during the exploration movement are illustrated in Fig. 7.

C. Weight

The goal of another experiment was to examine whether the sensor array modules could be used to acquire the weight of an object when grasped by a robot gripper. During the experiment the robot gripper was moved to the specified location of a cup on a table and established a grasp around

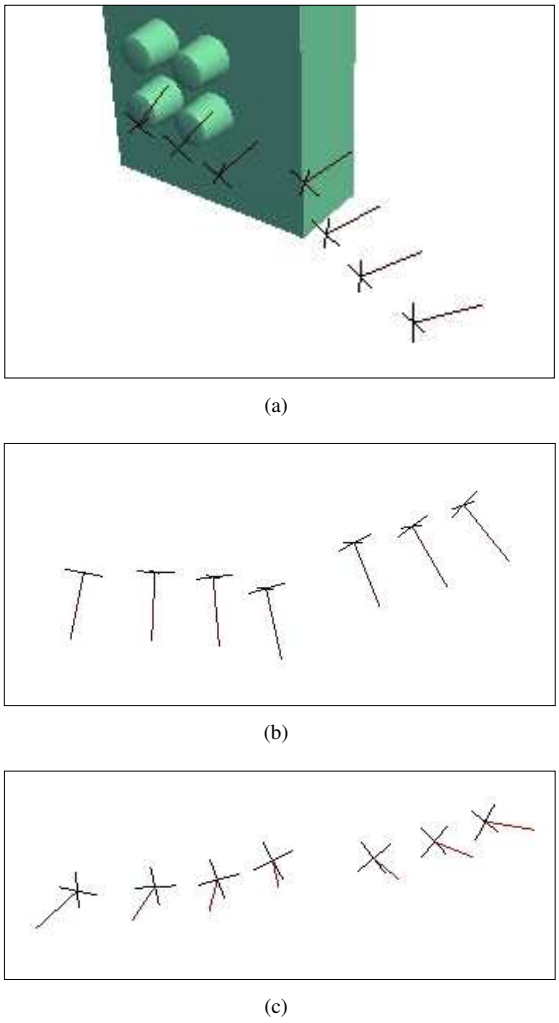

Fig. 7. Surface points found during the exploration of the bowl. The center of the cross marks the position. The red line marks the surface normal. **a)** Robot finger and exploration data as displayed in the control software during exploration. **b)** Surface points and normals seen from top view. **c)** Surface points and normals seen from the front.

it. The exploration procedure realized in the control program was to close the fingers slowly until the sensors could measure a minimum total contact force of 0.5 N from each sensor array, which is enough to provide a stable grasp. From here the object was slowly lifted 1 cm above the surface. The two phases of the experiment are illustrated in Fig. 8(a) and 8(b).

During the lifting phase a torque is applied to the actuation tips by the weight of the object which deforms the elastic material of the tips until an equilibrium is reached when the lifted object has completely left the supporting table.

The sensor values were acquired before and after lifting. The axis through the N- and S-subsensors was aligned to the lifting direction, therefore the difference of the corresponding readings $d = s - n$ was evaluated for examining the influence of the weight on the measurement values. The weight of the cup was increased during several measurements by filling the cup with metal items.

The mean difference over the N-S subsensor pairs of

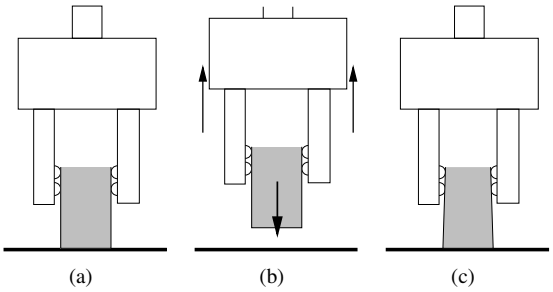

Fig. 8. Feature extraction experiments with the *MicroNav* sensor. **a)** The object is initially placed on the table. **b)** In the weight experiment a grasp is established and the object is lifted. **c)** In the elasticity experiment the object is compressed by the fingers.

all sensor elements for all tested weights is plotted in Fig. 9. The dotted line is a first order approximation to the measurements minimizing the least squares error. The data in this experiment was acquired with a single measurement point for each weight.

For determining the precision we repeated the measurement with a weight of 400 g for 20 times. The standard deviation of this measurement value was found to be 0.22 N.

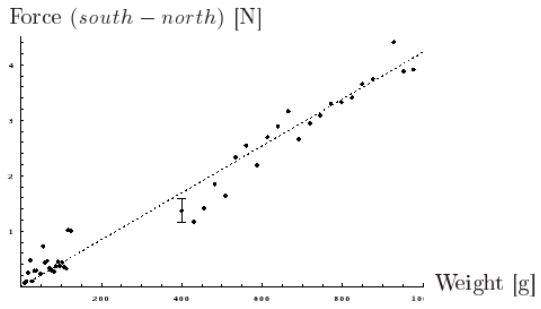

Fig. 9. Results of the *MicroNav* weight experiment

D. Elasticity

In a further experiment we investigated the sensor's ability to discriminate different elasticity values of an object. The same setup as in the preceding experiment was used with a different haptic exploration procedure.

A plastic cup was used as object under investigation, which could be squeezed by the gripper at different heights measured from the cups' bottom, see Fig. 8(c). Naturally, a plastic cup is more rigid close to the cup bottom than to the edge at the top. When pinched at the top, the profile of the plastic cup is deformed from a circular towards an oval shape.

The control program closed the parallel gripper slowly with a constant velocity and stopped when a certain force threshold was exceeded. This experiment was repeated five times at different contact locations along the body of the cup. A plot of the force measurement versus the distance decrement between the gripper fingers is shown in Fig. 10.

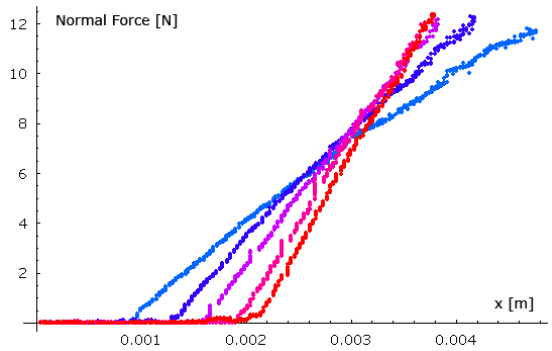

Fig. 10. Results of the elasticity experiment. Light Blue = grasp located at the top, Red = grasp located at the bottom, Other colors = grasp located in between

The plot exhibits a linear relationship which can be interpreted as accordance to Hooke's Law. The spring constant increases linear to larger values for locations closer to the cup bottom, which is reflected in the increasing slope of the plotted lines.[2]

To measure the precision of the elasticity measurements we evaluated the results of multiple measurements (11 times at the top and 16 times at the bottom). The distance traveled by the gripper fingers to reach a threshold force of 5 N is illustrated in Fig. 11. The results for the two measurement points clearly separate. This shows that it is possible to acquire local elasticity of an object using the developed procedure with a parallel gripper.

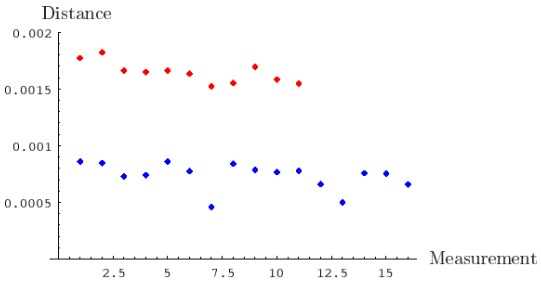

Fig. 11. Results of the *MicroNav* elasticity repeatability experiment. Red dots mark the measurements at the top of the cup. Blue dots mark the measurements at the bottom of the cup.

IV. Conclusions

In this work, we have investigated the potential of a sensor for the purpose of tactile sensing, which has been designed originally in the context of cursor navigation technology. The fact that this sensor is manufactured in mass production makes it cheap (less than 10 Euros per piece) and very robust. In contrast to most existing tactile sensors, it measures not only normal forces but also shear forces which is relevant for a number of applications such as weight measuring, slippage

[2]Note that the lines in Fig. 10 intersect with the x-axis at different coordinates as the diameter at the top edge of the cup is with 59 mm little larger compared to the the bottom with 57.5 mm.

detection, grasp optimization, etc. Also, individual sensors can be mounted in a very modular way to equip rather different grasping devices with tactile sensors. In addition, a high temporal resolution, a decent spatial resolution as well as a wide measurement range are interesting features of this sensor. We have demonstrated the potential of this sensorial framework for three different applications: Surface exploration, weight measurement and elasticity measurement.

As a summary, we believe that the sensors are an interesting alternative to existing tactile sensor systems due to the richness of information they provide, their low price and their modularity.

ACKNOWLEDGEMENT

The work described in this paper was conducted within the EU Cognitive Systems project PACO-PLUS (FP6-2004-IST-4-027657) funded by the European Commission.

APPENDIX

Our algorithm for shape exploration comprises three phases which are repeated in cyclic sequence:

1) Move robot finger in direction $\hat{n}$, normal to the sensor array, towards the object to be explored and stop when contact is detected, i.e. when the sensor readings exceed a given force threshold.
2) The sensor array must now become aligned with the tangential plane of the surface. During this phase two independent control loops are in operation. For this purpose only the average force readings of each of the four sensor elements are considered. The average force value f_m is calculated as the mean value of all four subsensors for each sensor element respectively. The center point of contact $\overrightarrow{p}$ can be calculated from the geometry of the sensor array and the force readings.
   First, a constant total force f_c, which is measured as the sum of the contact force values, must be maintained in order to keep the applied force of each individual sensor within a specified range. Using a PI velocity controller with coefficients $a_1,\ a_2$ this gives

$$\begin{aligned} e_n &= f_d - f_c \\ v_n &= a_1 e_n + a_2 \int e_n \end{aligned}$$

   with f_d as desired total force and v_n the velocity command in direction normal to the sensor array. This velocity is submitted to the robot arm controller.
   A second controller is required for performing the alignment of the sensor array to the surface normal by rotating around the array center point. The control error $\overrightarrow{e_r}$ is defined as the distance from the contact point location to the center of the sensor array $\overrightarrow{p_c}$. The sensor array is then rotated around the axis perpendicular to the normal vector $\hat{n}$ and $\overrightarrow{e_r}$ with angular velocity $\dot{\theta}$. The corresponding PI controller with coefficients $b_1,\ b_2$ is

$$\begin{aligned} \overrightarrow{e_r} &= \overrightarrow{p} - \overrightarrow{p}_c \\ \dot{\theta} &= b_1 \|e_r\| + b_2 \int \|e_r\| \quad . \end{aligned}$$

   When e_n and $\|e_r\|$ are minimal, the values of p_c and $\hat{n}$ are stored as surface point and normal for this step of the algorithm.
3) The finger is removed from the surface, so that it just releases contact and then moved a short distance in direction tangential to the previously acquired normal vector. From here the algorithm starts again at step 1.

REFERENCES

[1] Mark H. Lee and Howard Nicholls, "Tactile sensing for mechatronics - a state of the art survey," *Mechatronics*, vol. 9, pp. pp.1–31, 1999.
[2] T. Asfour, K. Regenstein, P. Azad, J. Schroder, A. Bierbaum, N. Vahrenkamp, and R. Dillmann, "Armar-III: An Integrated Humanoid Platform for Sensory-Motor Control," in *Humanoid Robots, 2006 6th IEEE-RAS International Conference on*, Dec. 2006, pp. 169–175.
[3] S.I. Yaniger, "Force Sensing Resistors: A Review Of The Technology," in *Electro International, 1991*, April 16-18, 1991, pp. 666–668.
[4] Johan Tegin and Jan Wikander, "Tactile sensing in Intelligent Robotic Manipulation - A Review," *Industrial Robot*, vol. Vol. 32, no. 1, pp. 64–70, No. 1, February 2005, Emerald Group Publishing Limited.
[5] Javad Dargahi and Siamak Najarian, "Advances in tactile sensors design/manufacturing and its impact on robotics applications - a review," *Industrial Robot: An International Journal*, vol. 32, no. 14, pp. 268–281, 2005.
[6] Interlink Electronics, *Force Sensing Resistor Integration Guide*, v1.0 Rev. D, http://www.interlinkelectronics.com.
[7] Y. Ohmura, Y. Kuniyoshi, and A. Nagakubo, "Conformable and scalable tactile sensor skin for curved surfaces," in *Robotics and Automation, 2006. ICRA 2006. Proceedings 2006 IEEE International Conference on*, May 15-19, 2006, pp. 1348–1353.
[8] Jun Ueda, Y. Ishida, M. Kondo, and T. Ogasawara, "Development of the NAIST-Hand with Vision-based Tactile Fingertip Sensor," in *Robotics and Automation, 2005. ICRA 2005. Proceedings of the 2005 IEEE International Conference on*, 18-22 April 2005, pp. 2332–2337.
[9] Antonio Bicchi, J. Kenneth Salisbury, and David L. Brock, "Contact Sensing from Force Measurements," *The International Journal of Robotics Research*, vol. Vol 12(3), no. 3, pp. 249–262, 1993.
[10] Jong-Ho Kim, Jeong-Il Lee, Hyo-Jik Lee, Yon-Kyu Park, Min-Seok Kim, and Dae-Im Kang, "Design of Flexible Tactile Sensor Based on Three-Component Force and Its Fabrication," in *Robotics and Automation, 2005. ICRA 2005. Proceedings of the 2005 IEEE International Conference on*, 18-22 April 2005, pp. 2578–2581.
[11] Lucia Beccai, Stefano Roccella, Alberto Arena, Francesco Valvo, Pietro Valdastri, Arianna Menciassi, Maria Chiara Carrozza, and Paolo Dario, "Design and fabrication of a hybrid silicon three-axial force sensor for biomechanical applications," *Sensors and Actuators A: Physical*, vol. 120, no. 2, pp. 370–382, 2005.
[12] Interlink Electronics, *MicroNav Integration Guide*, v3.0, http://www.interlinkelectronics.com.
[13] A. Kargov, T. Asfour, C. Pylatiuk, R. Oberle, H. Klosek, S. Schulz, K. Regenstein, G. Bretthauer, and R. Dillmann, "Development of an anthropomorphic hand for a mobile assistive robot," in *Rehabilitation Robotics, 2005. ICORR 2005. 9th International Conference on*, 28 June-1 July 2005, pp. 182–186.
[14] David J. Montana, "The kinematics of contact and grasp," *International Journal of Robotics Research*, vol. 7, no. 3, pp. 17 – 32, June 1988.